Zhao et al. *Zool. Res.* 2023, 44(6): 1015−1025
https://doi.org/10.24272/j.issn.2095-8137.2023.187

ZR | Zoological Research

Article Open Access

Cross-species recognition of bat coronavirus RsYN04 and cross-reaction of SARS-CoV-2 antibodies against the virus

Runchu Zhao[1,2,#], Sheng Niu[3,#], Pu Han[2,#], Yue Gao[2,4], Dezhi Liu[1,2], Chunliang Luo[2,3], Honghui Liu[2], Bo Liu[2,3], Yanli Xu[5], Jianxun Qi[2], Zhihai Chen[5], Weifeng Shi[6], Lili Wu[2,*], George F. Gao[2,7], Qihui Wang[1,2,7,*]

[1] *Institute of Physical Science and Information*, *Anhui University*, *Hefei*, *Anhui* 230039, *China*

[2] *CAS Key Laboratory of Pathogen Microbiology and Immunology*, *Institute of Microbiology*, *Chinese Academy of Sciences*, *Beijing* 100101, *China*

[3] *College of Veterinary Medicine*, *Shanxi Agricultural University*, *Jinzhong*, *Shanxi* 030801, *China*

[4] *School of Life Sciences*, *Hebei University*, *Baoding*, *Hebei* 071002, *China*

[5] *Center of Infectious Disease*, *Beijing Ditan Hospital*, *Capital Medical University*, *Beijing* 100015, *China*

[6] *Key Laboratory of Etiology and Epidemiology of Emerging Infectious Diseases in Universities of Shandong*, *Shandong First Medical University* & *Shandong Academy of Medical Sciences*, *Taian*, *Shandong* 271000, *China*

[7] *University of Chinese Academy of Sciences*, *Beijing* 100049, *China*

ABSTRACT

Following the outbreak of coronavirus disease 2019 (COVID-19), several severe acute respiratory syndrome coronavirus 2 (SARS-CoV-2)-related coronaviruses have been discovered. Previous research has identified a novel lineage of SARS-CoV-2-related CoVs in bats, including RsYN04, which recognizes human angiotensin-converting enzyme 2 (ACE2) and thus poses a potential threat to humans. Here, we screened the binding of the RsYN04 receptor-binding domain (RBD) to ACE2 orthologs from 52 animal species and found that the virus showed a narrower ACE2-binding spectrum than SARS-CoV-2. However, the presence of the T484W mutation in the RsYN04 RBD broadened its range. We also evaluated 44 SARS-CoV-2 antibodies targeting seven epitope communities in the SARS-CoV-2 RBD, together with serum obtained from COVID-19 convalescents and vaccinees, to determine their cross-reaction against RsYN04. Results showed that no antibodies, except for the RBD-6 and RBD-7 classes, bound to the RsYN04 RBD, indicating substantial immune differences from SARS-CoV-2. Furthermore, the structure of the RsYN04 RBD in complex with cross-reactive antibody S43 in RBD-7 revealed a potently broad epitope for the development of therapeutics and vaccines. Our findings suggest RsYN04 and other viruses belonging to the same clade have the potential to infect several species, including humans, highlighting the necessity for viral surveillance and development of broad anti-coronavirus countermeasures.

Keywords: SARS-CoV-2-related coronavirus; RsYN04; ACE2; Antibody; Structure

INTRODUCTION

Emerging and re-emerging pathogens pose a significant threat to global public health (Gao, 2018). Many viral pathogens in humans are of zoonotic origin, arising from either sporadic or frequent spillover infections from animals, with notable examples including coronaviruses (CoVs), Ebola virus, and avian influenza A virus. In particular, CoVs are known to infect a wide range of wild and domestic animals, and include porcine epidemic diarrhea virus (PEDV) (Pensaert & de Bouck, 1978), infectious bronchitis virus (IBV) (Fabricant, 1998), mouse hepatitis virus (MHV) (Weiner, 1973), bovine coronavirus (BCoV) (Bridger et al., 1978), canine coronavirus (CCoV) (Erles et al., 2003), feline coronavirus (FCoV) (Pedersen et al., 1984), Middle East respiratory syndrome coronavirus (MERS-CoV) (Zaki et al., 2012), severe acute respiratory syndrome coronavirus (SARS-CoV) (Ksiazek et al., 2003), and SARS-CoV-2 (Zhu et al., 2020). These viral infections have brought serious impact on animal and human health as well as economic development.

Exploring the origins and cross-species transmission patterns of these viruses is crucial for their prevention and control. Bats are suspected reservoir hosts for many CoVs (Wang et al., 2023), including SARS-CoV-2. In an effort to

Received: 24 August 2023; Accepted: 12 September 2023; Online: 13 September 2023

Foundation items: This work was supported by the National Key R&D Program of China (2022YFC2303403) and National Natural Science Foundation of China (82225021). Q.W. was supported by the Chinese Academy of Sciences (YSBR-010 and Y2022037)

[#]Authors contributed equally to this work

*Corresponding authors, E-mail: wulili@im.ac.cn; wangqihui@im.ac.cn

trace the origin of SARS-CoV-2, several highly SARS-CoV-2-related bat CoVs with >90% full-genome identity have been reported globally, including those detected in southern China (RaTG13) (Zhou et al., 2020b), Cambodia (RshSTT182 and RshSTT200) (Delaune et al., 2021), Japan (Rc-o139) (Murakami et al., 2020), Thailand (RacCS203) (Wacharapluesadee et al., 2021), and Laos (BANAL-52) (Temmam et al., 2022). In addition, a novel lineage of SARS-CoV-2-related CoVs in bats has been identified in southern China, including RsYN04 (identified from *Rhinolophus stheno*) and RaTG15 (identified from *R. affinis*), which share relatively low whole-genome identities (76.5% and 77.6%, respectively) with SARS-CoV-2 (Guo et al., 2021; Zhou et al., 2021). Notably, these bat CoVs have primarily been identified in the *Rhinolophus* genus, indicating potential role of these bats as reservoir hosts for SARS-CoV-2. Pangolin-origin SARS-CoV-2-related CoVs (e.g., GD/1/2019, GX/P2V/2017, and MP20) have also been suggested as potential contributors to the emergence of SARS-CoV-2 (Lam et al., 2020; Peng et al., 2021; Xiao et al., 2020). However, despite substantial global efforts in tracing the intermediate hosts and natural reservoirs of SARS-CoV-2, much remains unknown.

Receptor recognition is the first step for viral infection. Therefore, the gain-of-function of a virus to bind to the receptors in other species is a prerequisite for cross-species transmission. Studies from our group and others have demonstrated the broad receptor-binding spectra of SARS-CoV-2 and related CoVs, including RaTG13, GD/1/2019, GX/P2V/2017, and RshSTT182/200, by assessing the binding potency of their receptor-binding domains (RBDs) to angiotensin-converting enzyme 2 (ACE2) orthologs in different species (Damas et al., 2020; Hu et al., 2023; Liu et al., 2021b; Shi et al., 2020; Wu et al., 2020), highlighting their potential for cross-species spill over and infection in both animals and humans. Several animal species, such as cats, dogs, tigers, minks, and white-tailed deer, have been reported to be naturally infected by SARS-CoV-2 (Sharun et al., 2021), emphasizing the importance of investigating the cross-species infection of SARS-CoV-2 and related CoVs. Notably, although belonging to a novel lineage with very low sequence identity with SARS-CoV-2, RsYN04 still displays the binding capacity to human ACE2 (hACE2), thereby posing a potential threat to humans (Zhou et al., 2021). However, Guo et al. (2021) found that RaTG15 showed no detectable binding to hACE2 in their experimental system, indicating there is a limited potential for these viruses to infect humans. Nonetheless, compared to SARS-CoV-2 and other related CoVs, the potential difference in host recognition of this novel lineage of viruses is yet to be elucidated. Moreover, given the persistent public health challenge posed by COVID-19, elucidating the potential cross-species transmission of SARS-CoV-2-related CoVs is essential to help prevent future outbreak.

In this study, we selected RsYN04 as a representative of the novel lineage of SARS-CoV-2-related bat CoVs to examine its potential for cross-species infection and cross-reactive immune responses with SARS-CoV-2. Potential RsYN04 infection was first evaluated by examining the binding affinity of the RsYN04 RBD to ACE2s from different animal species. Furthermore, the cross-binding of serum from COVID-19 convalescents and vaccinees as well as seven classes of SARS-CoV-2 RBD-directed antibodies to the RsYN04 RBD was evaluated (Hastie et al., 2021; Huang et al., 2022). Subsequently, a broad epitope was identified via structural analysis of the RsYN04 RBD with a broad RBD-7 antibody S43. The findings of this study suggest that the bat CoV RsYN04, and viruses belonging to the same branch, possess the potential to infect several species, underscoring the importance of developing broad anti-CoV countermeasures against potential spillovers.

MATERIALS AND METHODS

Cells

HEK293F cells were cultured in SMM 293-TII medium (Sino Biological, China) at 37 °C and 5% CO_2 with agitation at 140 r/min. HEK293T and BHK-21 cells were cultured in Dulbecco's Modified Eagle medium (DMEM) supplemented with 10% fetal bovine serum (FBS) at 37 °C and 5% CO_2.

Serum samples

Serum samples were obtained from COVID-19 convalescents admitted to Ditan Hospital, Beijing, China, and from volunteers who received a third immunization with the ZF2001® protein subunit vaccine. The studies were conducted and approved by the Ethics Committee of the Institute of Microbiology, Chinese Academy of Sciences, Beijing, China (Project Number: SQIMCAS2021149).

Gene cloning

The coding sequences of full-length ACE2 orthologs from 52 animals were synthesized and cloned into pEGFP-N1, while the extracellular domains of 14 ACE2s fused with the mouse immunoglobulin G (IgG) fragment crystallizable (Fc) domain were cloned into pCAGGS vectors, as reported previously (Niu et al., 2021; Wu et al., 2020). The coding sequences of SARS-CoV-2 RBD (residues 319–541, GISAID: EPI_ISL_402119), SARS-CoV-2 N-terminal domain (NTD) (residues 20–286, GISAID: EPI_ISL_402119), RsYN04 RBD (residues 309–527, GISAID: EPI_ISL_1699444), and mutated RsYN04 RBD (T484W) were cloned into pCAGGS vectors with a C-terminal six histidine tag. The coding sequence of nanobody S43 with a C-terminal six histidine tag was also cloned into the pCAGGS vector. The coding sequence of the variable region of each antibody was synthesized from the submitted amino acid sequences in the Protein Data Bank. The heavy chains were fused with the constant region of human IgG1, and the light chains were fused with either Igκ or Igλ. Both were cloned into the pCAGGS vector.

Protein expression and purification

Protein A affinity column (GE Healthcare, USA) purification followed by gel filtration using a Superdex^{TM} 200 10/300GL column (GE Healthcare, USA) was used to purify the 14 ACE2 proteins fused with the mouse IgG Fc domain, 44 antibodies, and human ACE2 proteins fused with the human Fc tag from HEK293F cell culture supernatants. The purified proteins were then stored in phosphate-buffered saline (PBS) buffer. SARS-CoV-2 RBD, SARS-CoV-2 NTD, RsYN04 RBD, RsYN04-T484W RBD, and S43 nanobody with His tag were purified from the HEK293F cell culture supernatants using a His-Trap Excel column (GE Healthcare, USA), followed by purification using a Superdex^{TM} 200 Increase 10/300 GL column (GE Healthcare, USA). The purified proteins were then stored in buffer (20 mmol/L Tris-HCl, pH 8.0, and 150 mmol/L NaCl).

Flow cytometry assay

For the binding assay, pEGFP-N1 plasmids containing 52 ACE2 orthologs were transfected into BHK-21 cells using

polyethylenimine (Alfa, USA) according to the manufacturer's instructions. The cells (2×10^5) were then collected 24 h after transfection, suspended in PBS (with 0.5% FBS), incubated with purified individual His-tagged proteins at a concentration of 20 μg/mL for 30 min at 37 °C, then thrice washed with PBS and further incubated with anti-His/APC antibodies (1:500, Miltenyi Biotec, Germany). After further washing, the cells were analyzed using a BD LSRFortessa flow cytometer (USA). Data analysis was performed using FlowJo v7.6 (TreeStar, USA).

The ability of antibodies to block binding between the RsYN04 RBD/RsYN04-T484W RBD and *R. stheno* ACE2 was assessed using flow cytometry. BHK-21 cells were transiently transfected with the pEGFP-N1-ACE2 expression plasmid for 24 h. A mixture containing RsYN04 RBD or RsYN04-T484W RBD (30 μg/mL) with serially diluted COVA1-16, EY6A, CR3022, H014, or S43-hFc antibodies (from 300 μg/mL to 2.34375 μg/mL) was incubated at 4 °C for 30 min before being added to the BHK-21 cells and incubated again at 37 °C for 30 min. Subsequently, the cells were thrice washed with PBS containing 0.5% FBS and stained with anti-His/APC antibodies (1:500, Miltenyi Biotec, Germany). After the final washing, the cells were analyzed using a BD LSRFortessa flow cytometer (USA). Data analysis was performed using FlowJo v7.6 (TreeStar, USA).

Enzyme-linked immunosorbent assay (ELISA)

The SARS-CoV-2 RBD and RsYN04 RBD proteins were diluted to a concentration of 2 μg/mL with 0.05 mol/L carbonate-bicarbonate buffer (pH 9.6), then coated onto 96-well ELISA plates for overnight incubation at 4 °C. The plates were blocked with 5% skim milk in PBS supplemented with Tween 20 (PBST) and incubated with serially diluted serum samples and 10 μg/mL monoclonal antibodies (MAbs). Each serum sample was prepared in triplicate. The plates were subsequently incubated with goat anti-human IgG-horseradish peroxidase (HRP) antibodies (Thermo Fisher, USA), then developed with 3,3',5,5'-tetramethylbenzidine (TMB) substrate. The reactions were stopped with 2 mol/L sulfuric acid. Absorbance was measured at 450 nm using a microplate reader (PerkinElmer, USA). The endpoint titer was defined as the highest reciprocal dilution of serum to achieve an absorbance greater than 2.1-fold that of background values.

Surface plasmon resonance (SPR) assay

The 14 ACE2-mFc fusion proteins were immobilized on a CM5 chip. Serially diluted RsYN04 RBD and RsYN04-T484W RBD proteins were then flowed over the chip in PBST buffer. The SARS-CoV-2 RBD protein was used as a positive control. Binding affinities were measured at 25 °C using the BIAcore 8K system (GE Healthcare, USA) in single-cycle mode. Binding kinetics were analyzed using BIAcore® 8K Evaluation Software (GE Healthcare, USA) with a 1:1 Langmuir binding model.

The five recombinant antibodies (1 μg/mL) were first captured on flow cell 2 of the protein A sensor chip (GE Healthcare, USA) at over 500 response units (RUs). Flow cell 1 was used as a negative control. Serially diluted SARS-CoV-2 RBD, RsYN04 RBD, and RsYN04-T484W RBD proteins were then flowed over the chip in PBST buffer. The RUs were measured using the BIAcore 8K system (GE Healthcare, USA) in single-cycle mode. Antibodies were regenerated with 10 mmol/L glycine-HCl (pH 1.5). Equilibrium dissociation constants (K_D) of each pair of interactions were calculated using BIAcore® 8K Evaluation Software (GE Healthcare, USA) with fitting to a 1:1 Langmuir binding model.

Crystal screening and structure determination

The sitting-drop method was used to obtain RsYN04 RBD-S43 complex crystals. In detail, purified complex proteins were concentrated to 12 mg/mL. After this, 0.8 μL of protein was mixed with 0.8 μL of reservoir solution. The resulting solution was sealed and equilibrated against 80 μL of reservoir solution at 18 °C. High-resolution RsYN04 RBD-S43 complex crystals were grown in 0.2 mol/L potassium nitrate and 20% (w/v) polyethylene glycol 3 350 (PEG 3 350).

Crystal diffraction data were obtained from the Shanghai Synchrotron Radiation Facility BL19U1 (wavelength, 0.97852 Å or 0.97853 Å) and processed using HKL2000 software (Otwinowski & Minor, 1997). The RsYN04 RBD-S43 complex crystal structures were obtained by molecular replacement using Phaser with a previously reported SARS-CoV-2 RBD-S43 complex structure (PDB:7KN5). Atomic models were completed with Coot (Emsley & Cowtan, 2004) and refined with phenix.refine in Phenix (Adams et al., 2002). The stereochemical qualities of the final models were assessed with MolProbity (Williams et al., 2018). Data collection, processing, and refinement statistics are summarized in Supplementary Table S1. All structural figures were prepared using Pymol software (http://www.pymol.org).

RESULTS

Cross-species recognition of RsYN04 to ACE2 orthologs from 52 species

To explore the potential of cross-species transmission of RsYN04, we selected 51 animal species, in addition to humans, covering most domestic animals and companion pets, and several wild animals, notably various bat species. The 51 animals belonged to 10 orders, including Primates (crab-eating macaque), Carnivora (cat, civet, dog, fox, raccoon dog, and American mink), Rodentia (mouse, rat, golden hamster, Chinese hamster, and guinea pig), Artiodactyla (bovine, pig, goat, sheep, wild Bactrian camel, and deer), Pholidota (Malayan pangolin), Perissodactyla (horse), Lagomorpha (rabbit), Galliformes (chicken), Afrosoricida (lesser hedgehog tenrec), and Chiroptera (including 19 *Rhinolophus* species and nine non-*Rhinolophus* species of bats) (Figure 1). The binding properties between RsYN04 RBD and ACE2 orthologs of these animals were assessed in comparison to SARS-CoV-2 RBD.

Flow cytometry indicated that the RsYN04 RBD could bind to the ACE2 orthologs from nine species, including Primates (human and crab-eating macaque), Carnivora (cat), Rodentia (golden hamster and Chinese hamster), Artiodactyla (bovine), Chiroptera (*Myotis davidii*, *R. affinis*, and *R. stheno*), a narrower range than that of SARS-CoV-2 RBD, which can bind to 34 ACE2 orthologs (Figure 1). Additionally, the binding affinity of RsYN04 for ACE2 orthologs was weaker than that of SARS-CoV-2, although RsYN04 RBD exhibited higher binding to *R. affinis* and especially to *R. stheno*, the natural host of RsYN04, compared to the other seven ACE2 orthologs.

Previous studies have indicated that the T484W mutation of RsYN04 RBD (homologous to Q498 in SARS-CoV-2) can enhance ACE2 ortholog binding, including in humans (Starr et al., 2022). Here, the RsYN04-T484W RBD exhibited stronger binding to the nine ACE2 orthologs than the wild-type RsYN04 RBD, and acquired the ability to bind to the pig, goat,

Figure 1 Characterization of binding of 52 ACE2s with RsYN04 RBD, RsYN04-T484W RBD, and SARS-CoV-2 RBD by flow cytometry

His-tagged RsYN04 RBD, RsYN04-T484W RBD, and SARS-CoV-2 RBD proteins were incubated with BHK-21 cells expressing eGFP-fused ACE2. SARS-CoV-2 NTD was used as a negative control. Anti-His/APC antibody was used to detect cells binding with His-tagged protein. One representative result from two independent experiments with two replicates (n=2) is shown. Cells stained with RsYN04 RBD, RsYN04-T484W RBD, SARS-CoV-2 RBD, and SARS-CoV-2 NTD proteins are shown in upper left, upper right, lower left, and lower right, respectively. Species with cross-binding are in blue.

sheep, rabbit, and *R. sinicus WJ1* ACE2 orthologs (Figure 1). These findings indicate that RsYN04 has the potential to infect these animals, especially when T484 mutates to W484.

The binding affinities of the RsYN04 and RsYN04-T484W RBDs to the 14 ACE2 orthologs were further evaluated using SPR assays (Figure 2). The affinities of the ACE2s to RsYN04 RBD were predominantly at the micromolar level, which is less than the nanomolar level observed for the SARS-CoV-2 RBD. Although the RsYN04-T484W RBD exhibited enhanced ACE2 binding ability in most species, its affinity for human, *R. stheno*, *R. affinis*, and *M. davidii* orthologs demonstrated no significant differences (<3-fold) compared to the wild-type RsYN04 RBD. Notably, the RsYN04 RBD displayed a 20-fold stronger affinity to the *R. stheno* ACE2 than to hACE2 (0.69±0.17 μmol/L versus 14.76±0.11 μmol/L). Consistent with flow cytometry, no interactions were observed between the RsYN04 RBD and ACE2 orthologs of rabbit and pig. In contrast, the SPR assay results indicated that the RsYN04

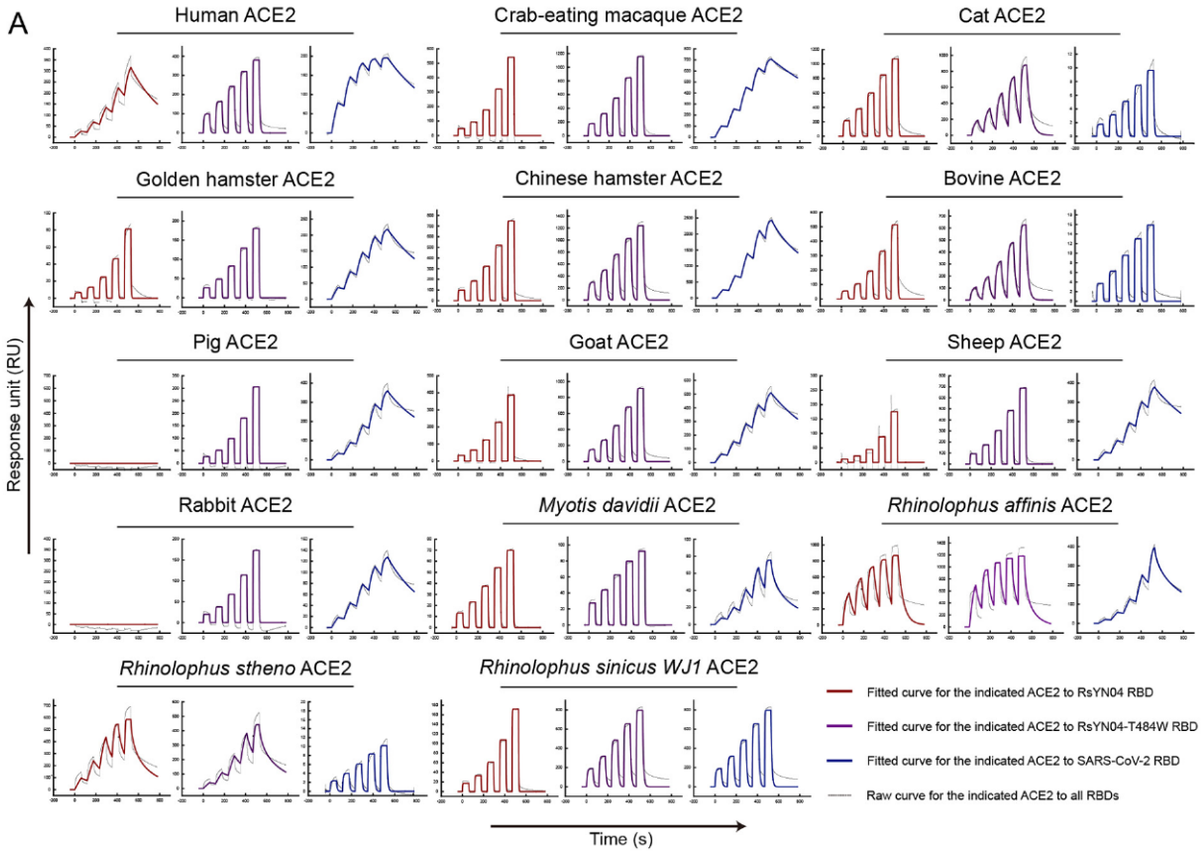

B

	RsYN04 RBD (μmol/L)	RsYN04-T484W RBD (μmol/L)	SARS-CoV-2 RBD (μmol/L)
Human	14.76±0.11	9.39±0.12	0.04±0.04
Crab-eating macaque	>202.60±40.00	22.59±0.84	0.01±0.0001
Cat	35.73±0.91	2.54±0.15	0.06±0.03
Golden hamster	>219.73±82.21	27.57±2.54	0.01±0.01
Chinese hamster	75.02±3.03	10.27±0.40	0.02±0.001
Bovine	>122.07±1.51	4.18±0.6	0.07±0.04
Pig	—	>102.15±18.20	0.02±0.004
Goat	>265.67±52.54	20.58±0.38	0.02±0.0009
Sheep	>3806.97±2143.62	28.32±0.86	0.02±0.003
Rabbit	—	40.52±1.97	0.01±0.003
Myotis davidii	8.87±1.56	7.99±0.56	0.04±0.005
Rhinolophus affinis	1.54±0.22	0.55±0.14	0.05±0.01
Rhinolophus stheno	0.69±0.17	0.28±0.03	0.11±0.08
Rhinolophus sinicus WJ1	>149.76±7.56	11.78±3.22	0.04±0.01

Figure 2 Binding affinity between ACE2s and RsYN04 RBD, RsYN04-T484W RBD, and SARS-CoV-2 RBD by SPR assay

A: mFc-tagged ACE2s were immobilized on a CM5 chip, followed by sequential testing of binding with serially diluted RsYN04 RBD, RsYN04-T484W RBD, and SARS-CoV-2 RBD. Raw and fitted curves are displayed as dotted and solid lines, respectively. B: Binding affinities between RBDs (RsYN04 RBD, RsYN04-T484W RBD and SARS-CoV-2 RBD) and 14 ACE2s are shown as mean±standard deviation (*SD*) of three independent experiments. "–" indicates not determined.

RBD was able to weakly bind to the ACE2 orthologs of goat, sheep, and *R. sinicus WJ1*, potentially due to the different sensitivities of the detection methods. The T484W mutant was able to bind to all 14 tested ACE2s, implying that the mutation plays a vital role in viral cross-species transmission.

Cross-reactive immune response of SARS-CoV-2 to RsYN04

To assess the immunological cross-reactivity between RsYN04 and SARS-CoV-2, the cross-binding antibodies in serum samples obtained from COVID-19 convalescents (infected by the SARS-CoV-2 prototype) and vaccinees (received the three-dose ZF2001® vaccine) were first analyzed against the RsYN04 RBD using ELISA. Results indicated that SARS-CoV-2 antibodies present in the sera of all convalescent donors and vaccinees were able to cross-recognize the RsYN04 RBD, achieving an endpoint titer ranging from 10^3 to 10^5. Furthermore, no significant difference was observed in the antibody titers binding to RsYN04 RBD and those binding to SARS-CoV-2 RBD (Figure 3). Moreover, the RsYN04 RBD-specific antibody levels of vaccinees induced by the three-dose ZF2001® vaccine were slightly higher than those observed in COVID-19 convalescent donors.

A total of 44 SARS-CoV-2 MAbs divided into seven communities (RBD-1 to RBD-7) based on their RBD epitope

were chosen to test their binding capacities to RsYN04 RBD by ELISA (He et al., 2023; Huang et al., 2022). Among the antibodies, all 38 antibodies belonging to RBD-1, RBD-2, RBD-3, RBD-4, and RBD-5 communities lost their binding ability to the RsYN04 RBD (Figure 4A). However, six antibodies in the RBD-6 and RBD-7 groups displayed variable binding to the RsYN04 RBD. Notably, CR3022, EY6A, H014, and our previously reported antibody S43 (Liu et al., 2023) in RBD-7 retained similar binding ability to RsYN04 RBD as to SARS-CoV-2 RBD, whereas COVA1-16 in RBD-6 and S2A4 in RBD-7 decreased or lost their binding abilities to RsYN04 RBD.

The binding affinities of antibodies that maintained binding strength to the RsYN04 RBD were detected using SPR assay (Figure 4B). COVA1-16 in RBD-6 exhibited an approximate 16-fold lower affinity to the RsYN04 RBD than to the SARS-CoV-2 RBD. CR3022, EY6A, and H014 in RBD-7 showed comparable binding capacities to the RsYN04 RBD and SARS-CoV-2 RBD. Although S43 exhibited an approximate 10-fold decrease in binding affinity to the RsYN04 RBD than to the SARS-CoV-2 RBD, its binding strength remained relatively high, with an equilibrium dissociation constant (K_D) value of 0.2 nmol/L. These findings suggest that RBD-6 and RBD-7 serve as effective epitopes for this lineage of SARS-CoV-2-related viruses. Further examination using flow cytometry was conducted to examine whether these combinative antibodies could inhibit recognition of the RsYN04 RBD to *R. stheno* ACE2. Both H014 and S43 completely blocked the binding of the RsYN04 RBD to ACE2, while COVA1-16, CR3022, and EY6A partially inhibited this binding, even at a maximum concentration of 300 μg/mL (Supplementary Figure S1). Nevertheless, in the presence of COVA1-16, CR3022, or EY6A, the occurrences of RsYN04 RBD binding to *R. stheno* ACE2 decreased in an antibody concentration-dependent manner. These results indicate that RBD-7 antibodies, especially H014 and S43, possess a robust capability to block viral entry.

RsYN04 RBD and MAb S43 complex structure

We previously clarified the molecular basis of the binding of MAb S43 to the SARS-CoV-2 RBD (Liu et al., 2023). To shed light on the functional mechanism underlying the cross-reactivity of S43, we determined the RsYN04 RBD-S43 complex structure at a resolution of 3.0 Å (Supplementary Table S1). Overall, the RsYN04 RBD-S43 complex structure is similar to SARS-CoV-2 RBD-S43, with a root-mean-square deviation (RMSD) of 0.563 Å (for 269 Cα atoms) (Figure 5A), indicating that the two phylogenetically related CoV RBDs have highly conserved structures and similar modes of interaction with S43. Notably, there are four amino acids deletions (K444, V445, G446, and G447) were detected in the α4β7 loop region of the RsYN04 RBD compared to the SARS-CoV-2 RBD (Figure 5B, D).

S43, belonging to RBD-7, targets the inner face of the SARS-CoV-2 RBD and binds away from the receptor-binding motif (RBM) but can block ACE2 binding due to ACE2 glycosylation (Liu et al., 2023). Similarly, by superimposing the RsYN04 RBD-S43 complex onto the SARS-CoV-2 RBD-hACE2 complex (PDB code: 6LZG) (Wang et al., 2020), we found that this antibody exhibited steric hindrance with the N322 glycan of hACE2, although there was no overlap with the ACE2-binding site at the S43 epitope (Figure 5C, D). Hence, the inhibitory effect of S43 on the interaction between the RsYN04 RBD and ACE2 receptor is likely attributed to the N322 glycosylation of ACE2s, a relatively conserved feature among animal species (Supplementary Figure S2).

Key residues contributing to the hydrogen bond and van der Waals (vdw) interaction between the RsYN04 RBD and S43 were labeled (Figure 6A; Supplementary Table S2). Overall, 16 residues in the S43 paratope interacted with the RsYN04 RBD, 14 of which were derived from complementarity-determining region (CDR) 3 and only two from framework region (FR) 2. Total interactions between S43 and the RsYN04 RBD and SARS-CoV-2 RBD were 129 and 123, including eight and 12 hydrogen bonds, respectively (Figure 6A–D; Supplementary Table S2). Compared to SARS-CoV-2, Y359, T366, F367, and D417 in the RsYN04 RBD lost hydrogen bond interactions with S43 Y107, T112, T108, and S102, respectively. We next focused on the four RBD substitutions at the S43 binding interface, namely R368/K378, S403/G413, Q489/V503, and D490/G504 (Figure 5D). R368 in RsYN04 showed comparable binding to S43 as K378 in SARS-CoV-2 (Figure 6A–D; Supplementary Table S2). Compared to G413 in SARS-CoV-2, S403 in RsYN04 impaired the hydrophobic interactions with Y101 in S43. Both Q489 and D490 broke the hydrophobic interaction with W111

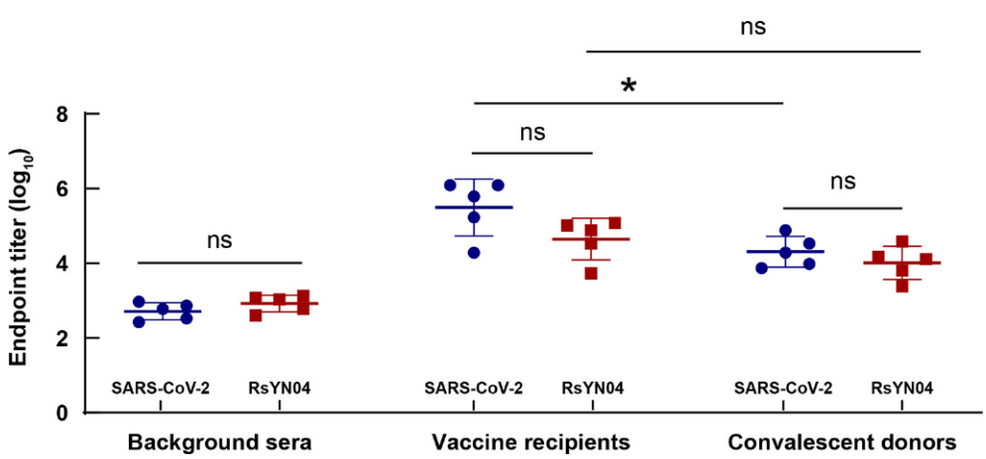

Figure 3 Binding activities of serum from ZF2001® vaccinees and COVID-19 convalescent donors to RsYN04 RBD

ELISA showing IgG titers of serum from ZF2001® vaccinees, COVID-19 convalescent donors, and unvaccinated individuals (background) against RsYN04 RBD or SARS-CoV-2 RBD. One representative result from two independent experiments is shown (n=3). Statistical analysis was performed via unpaired two-tailed t-test. ns: Not significant; *: P<0.05.

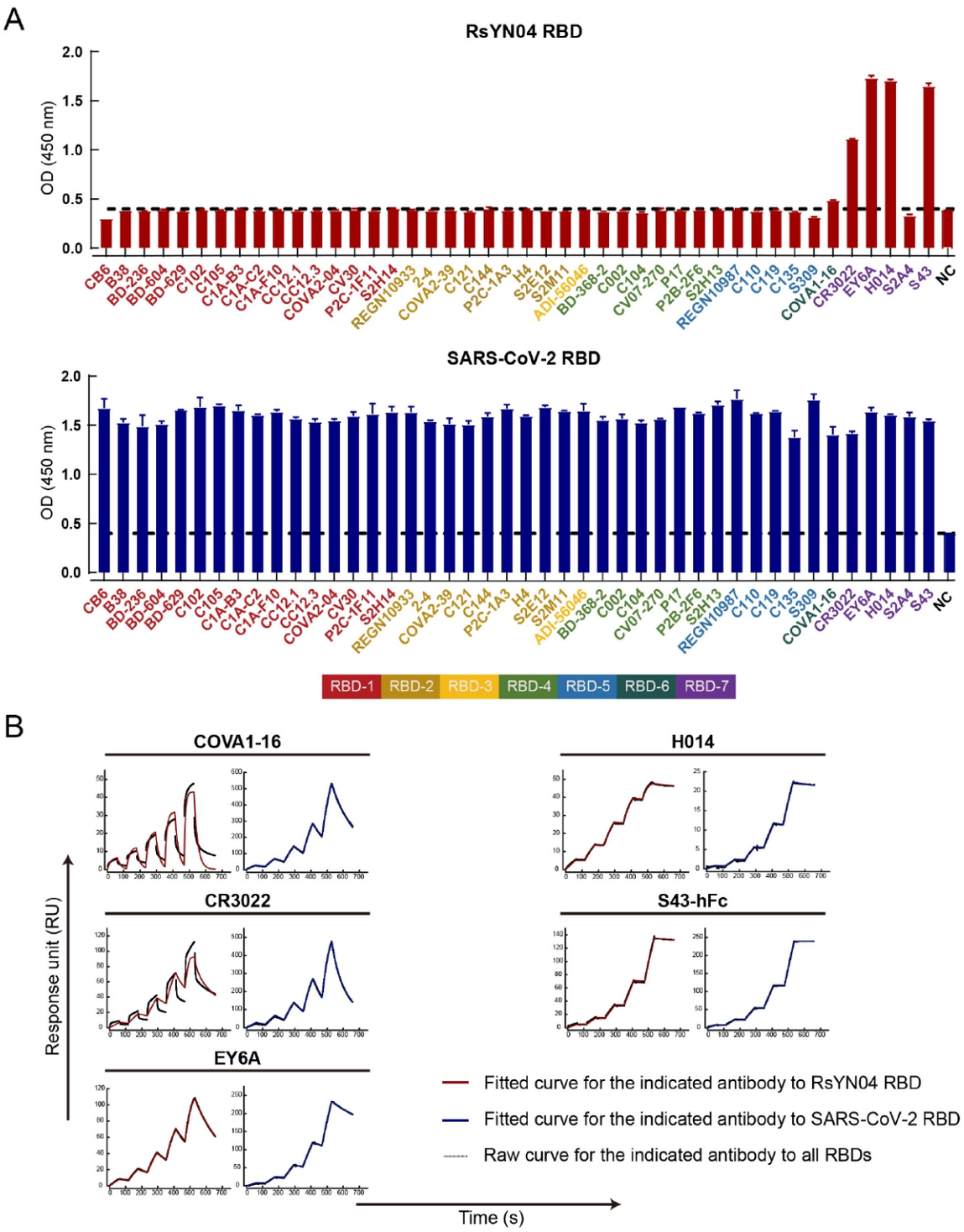

		Binding affinity (*K*D: nmol/L)	
Class	**Abs**	**RsYN04 RBD**	**SARS-CoV-2 RBD**
RBD-6	COVA1-16	730.0±270.0	46.8±8.9
RBD-7	CR3022	66.6±27.6	35.0±6.5
RBD-7	EY6A	10.8±2.0	3.3±2.0
RBD-7	H014	1.6±0.33	2.0±0.4
RBD-7	S43-hFc	0.2±0.2	0.02±0.006

Figure 4 Characterization of RsYN04 RBD binding to seven epitope classes of SARS-CoV-2 antibodies

A: ELISA of binding capacities of 44 SARS-CoV-2 antibodies to RsYN04 RBD and SARS-CoV-2 RBD. B: SPR analysis of binding affinities of SARS-CoV-2 antibodies to RsYN04 RBD and SARS-COV-2 RBD. Raw and fitted curves are displayed as dotted and solid lines, respectively. Data are shown as mean±standard deviation (*SD*) of three independent experiments.

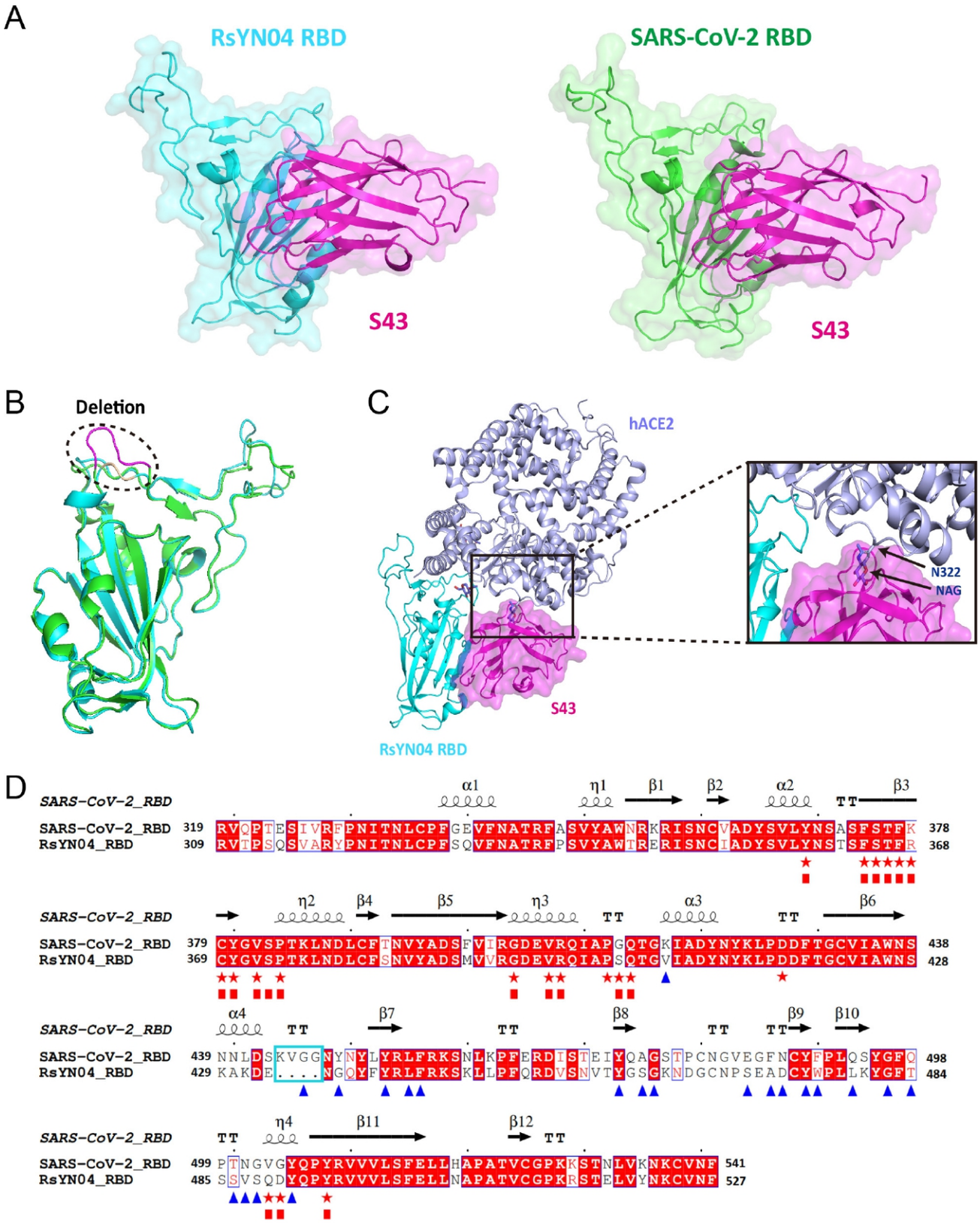

Figure 5 Complex structure of RsYN04 RBD and antibody S43

A: Overall structures of RsYN04 RBD-S43 and SARS-CoV-2 RBD-S43 complexes. SARS-CoV-2 RBD, RsYN04 RBD, and S43 are shown in green, cyan, and magenta, respectively. B: Structural comparison between RsYN04 RBD and SARS-CoV-2 RBD. Deletion of RsYN04 RBD compared to SARS-CoV-2 RBD is circled. C: Comparison between S43 binding to RsYN04 RBD and human ACE2 (hACE2) binding to RsYN04 RBD. Glycosylated residue N322 of hACE2 is framed and magnified. D: Sequence alignment of RBD sequences from RsYN04 and SARS-CoV-2. Blue triangles indicate binding sites of SARS-CoV-2 to hACE2. Red pentagrams indicate binding sites of SARS-CoV-2 RBD to S43, and red rectangles indicate binding sites of RsYN04 RBD to S43.

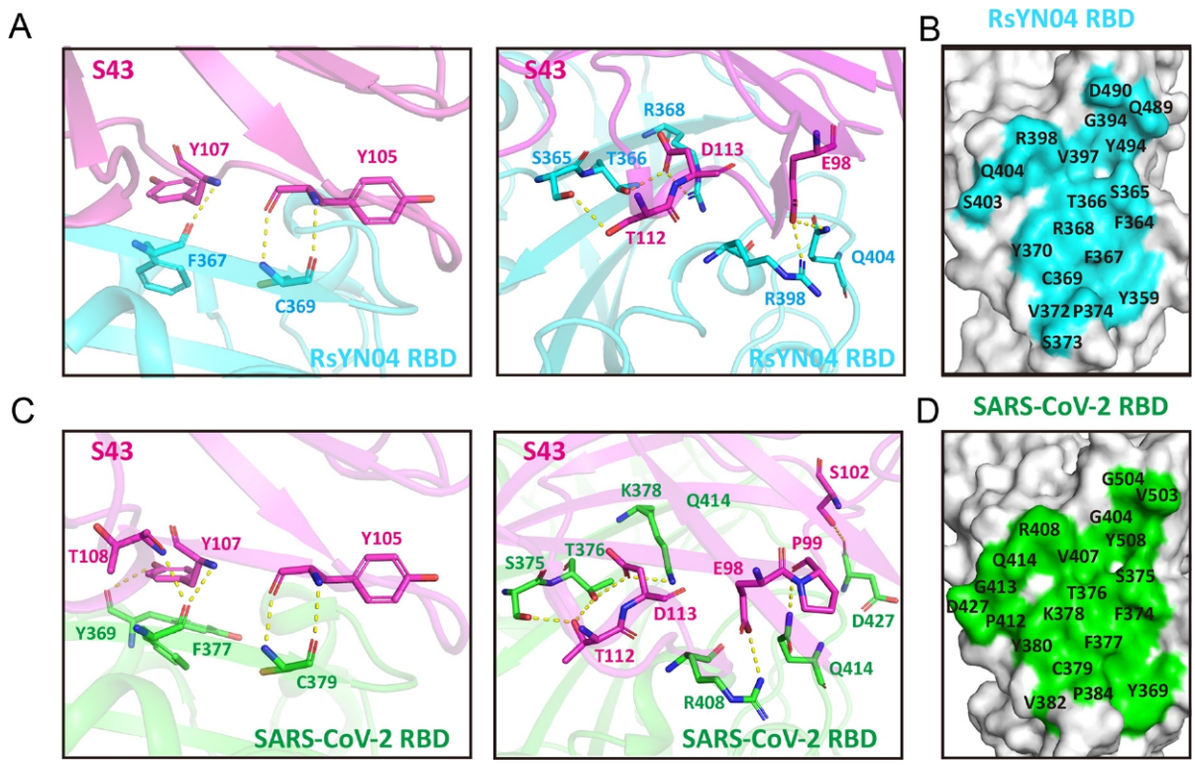

Figure 6 Detailed analysis of S43 interacting with RsYN04 RBD

A: Detailed interactions of RsYN04 RBD with S43. Hydrogen bonds are shown as yellow dotted lines with a cutoff of 3.3 Å. B: Structure of RsYN04 RBD is displayed in surface view. Residues that interact with S43 are marked. C: Detailed interactions of SARS-CoV-2 RBD with S43. Hydrogen bonds are shown as yellow dotted lines with a cutoff of 3.3 Å. D: Structure of SARS-CoV-2 RBD is displayed in surface view. Residues that interact with S43 are marked.

in S43, although they enhanced hydrophilic interactions with E44 and R45, respectively. Thus, we speculate that the decreased hydrogen bonds and hydrophobic interaction between S43 and RsYN04 RBD probably resulted in the observed ~10-fold lower binding compared to S43 with SARS-CoV-2 RBD (Figure 4B).

DISCUSSION

Since the COVID-19 outbreak, a wide variety of bats have been investigated to identify potential reservoirs of SARS-CoV-2, and various bat CoVs have been detected (Guo et al., 2021; Temmam et al., 2022; Wong et al., 2020; Zhou et al., 2020a, 2020b, 2021). A novel lineage of bat CoVs, including RsYN04, utilizes the same receptor as SARS-CoV-2 and SARS-CoV (Liu et al., 2021a; Temmam et al., 2022), posing a potential threat to public health. Therefore, it is necessary to evaluate the risk of cross-species transmission and prepare countermeasures against these CoVs.

Analyzing the interaction between the RBDs of viruses and ACE2 orthologs from various animals, including humans, offers a viable method to estimate the potential for cross-species transmission of SARS-CoV-2 and related CoVs (Castiglione et al., 2021; Damas et al., 2020; Liu et al., 2021a; Niu et al., 2021). In the current study, we applied a similar strategy to assess the potential ACE2-binding spectra of RsYN04, which exhibits lower whole-genome sequence (76.5%) and RBD-region identity (65.1%) to SARS-CoV-2 than to other bat CoVs, such as RaTG13 and RshSTT182. Our results showed that RsYN04 displayed a narrower host range than SARS-CoV-2. Furthermore, the binding ability of the RsYN04 RBD to ACE2 orthologs was also lower than that of the SARS-CoV-2 RBD, highlighting their evolutionary divergence. This disparity between RsYN04 and SARS-CoV-2 may be due to sequence divergence, particularly the distinctive deletion in the RsYN04 RBM. A comparable deletion has also been observed in the RshSTT182 RBD, with its repairation significantly enhancing binding affinity to hACE2 (Hu et al., 2023).

Mutation and recombination are fundamental drivers for viral evolution. We previously reported that the SARS-CoV-2 RBD bearing the Q498H mutation exhibits enhanced hACE2 binding, with extended mouse, rat, and European hedgehog ACE2 binding, attributed to the increased positive charge and larger side chain of histidine (H) (Supplementary Figure S3A, B) (Niu et al., 2021). Here, our results showed that the introduction of the T484W mutation in the RsYN04 RBD also improved its binding affinity to several animal ACE2 orthologs. This mutation also enabled binding to pig, goat, sheep, rabbit, and *R. sinicus WJ1* ACE2s. The improved binding was primarily attributed to the larger side chain and increased hydrophobicity of tryptophan (W), thus enhancing its interaction with ACE2 (Supplementary Figure S3C). These findings not only underscore the importance of the T484 site during viral evolution to facilitate cross-species transmission but also increase concerns regarding potential cross-species transmission of bat CoV RsYN04 and other viruses belonging to the same cluster, posing a threat to their relatively broad range of hosts, including humans. Therefore, continuous surveillance and retrospective research on animals and humans residing in *R. stheno* habitats, such as Southeast Asia, are imperative.

Given the potential threat, it is crucial to determine whether existing vaccines or treatments developed against SARS-

CoV-2 can prevent or combat possible disease caused by RsYN04. In our recent studies, ZF2001® vaccination and SARS-CoV-2 infection were shown to induce strong cross-reactive antibodies to related CoVs, including bat CoVs (RaTG13 and RshSTT182) and pangolin CoVs (GX/P2V/2017) (Hu et al., 2023; Jia et al., 2022). Similarly, in the current study, we found that ZF2001® vaccination and SARS-CoV-2 infection also induced cross-binding antibodies to the RsYN04 RBD. Furthermore, all tested SARS-CoV-2 MAbs assigned to the RBD-1 to RBD-5 epitope classes demonstrated a loss of binding to the RsYN04 RBD, indicating different antigenicity between the SARS-CoV-2 RBD and RsYN04 RBD. COVA1-16, the only RBD-6 member, exhibited decreased affinity for the RsYN04 RBD. However, four of the five RBD-7 antibodies were able to bind to the RsYN04 RBD with similar or slightly lower affinities than those to the SARS-CoV-2 RBD, suggesting that RBD-7 is a broad epitope. Further sequence analysis indicated that compared to SARS-CoV-2, the RsYN04 RBD contained only three substitutions in the RBD-6 and RBD-7 epitopes but more than forty substitutions in the binding sites of RBD-1 to RBD-5 (Supplementary Figure S4), suggesting that RBD-6 and RBD-7 may be broad epitopes for drug and vaccine development against SARS-CoV-2-related CoVs. However, the conformation of viral S-trimer should also be considered in drug and vaccine design given its importance in the effectiveness of these countermeasures (He et al., 2023). Additionally, peptide fusion inhibitors with pan-coronavirus inhibitory activity, such as our recently reported HY3000 (Wu et al., 2023), currently have been finished Phase II clinical trial in China, should be evaluated in future studies for their efficacy against SARS-CoV-2-related viruses.

LIMITATIONS OF THE STUDY

Our results suggested a wide ACE2-binding spectrum of RsYN04 but did not conclusively prove the susceptibility of species, whose ACE2 can bind to RsYN04 RBD. Thus, further studies, using live RsYN04 if available, are needed to evaluate the susceptibility of different species to this virus. In addition, although ZF2001® vaccination and SARS-CoV-2 infection induced cross-binding antibodies to RsYN04, the level of binding antibodies may not be consistent with that of neutralizing antibodies. For example, the neutralizing activities of sera for GX/P2V/2017 significantly decreased despite similar levels of binding antibodies (Jia et al., 2022). Therefore, the antiviral potency of serum following ZF2001® vaccination and SARS-CoV-2 infection, as well as MAbs recognizing RBD-6 and RBD-7 and peptide fusion inhibitors against RsYN04, should be evaluated in future studies.

DATA AVAILABILITY

The atomic coordinates for the RsYN04 RBD-S43 complex crystal structure were deposited in the Protein Data Bank (www.rcsb.org) (PDB ID code 8J5J).

SUPPLEMENTARY DATA

Supplementary data to this article can be found online.

COMPETING INTERESTS

Q.W., G.F.G., H.L., B.L., and L.W. are listed as coinventors of the patent for the antibody S43. G.F.G. is the holder of the patent intellectual property for the ZF2001® vaccine.

AUTHORS' CONTRIBUTIONS

G.F.G. and Q.W. initiated and coordinated the project and designed the experiments. R.Z., Y.G., and D.L. performed the SPR and FACS analyses with help from L.W. and C.L. R.Z. and S.N. prepared the RsYN04 RBD-S43 crystals with help from H.L. and B.L. P.H. and J.Q. solved the structure. Z.C. and Y.X. provided the serum samples. W.S. provided the ACE2 sequence of *R. stheno*. R.Z., S.N., L.W., G.F.G., and Q.W. analyzed the data and wrote the manuscript. All authors read and approved the final version of the manuscript.

ACKNOWLEDGMENTS

We are grateful to T. Zhao (Institute of Microbiology, Chinese Academy of Sciences (CAS)) for supporting the flow cytometry assay. We are grateful to Y. Chen (Institute of Biophysics, CAS) and Z. Fan (Institute of Microbiology, CAS) for their technical support for SPR analysis. We also thank K. Liu and L. Li (Institute of Microbiology, CAS) for providing the SPR assay method. We acknowledge the staff and beamline experts of BL19U1 at the Shanghai Synchrotron Radiation Facility for assistance during data collection.

REFERENCES

Adams PD, Grosse-Kunstleve RW, Hung LW, et al. 2002. *PHENIX*: building new software for automated crystallographic structure determination. *Acta Crystallographica Section D*: *Biological Crystallography*, **58**(Pt 11): 1948–1954.

Bridger JC, Caul EO, Egglestone SI. 1978. Replication of an enteric bovine coronavirus in intestinal organ cultures. *Archives of Virology*, **57**(1): 43−51.

Castiglione GM, Zhou LL, Xu ZH, et al. 2021. Evolutionary pathways to SARS-CoV-2 resistance are opened and closed by epistasis acting on ACE2. *PLoS Biology*, **19**(12): e3001510.

Damas J, Hughes GM, Keough KC, et al. 2020. Broad host range of SARS-CoV-2 predicted by comparative and structural analysis of ACE2 in vertebrates. *Proceedings of the National Academy of Sciences of the United States of America*, **117**(36): 22311−22322.

Delaune D, Hul V, Karlsson EA, et al. 2021. A novel SARS-CoV-2 related coronavirus in bats from Cambodia. *Nature Communications*, **12**(1): 6563.

Emsley P, Cowtan K. 2004. *Coot*: model-building tools for molecular graphics. *Acta Crystallographica Section D*: *Biological Crystallography*, **60**(Pt 12 Pt 1): 2126–2132.

Erles K, Toomey C, Brooks HW, et al. 2003. Detection of a group 2 coronavirus in dogs with canine infectious respiratory disease. *Virology*, **310**(2): 216−223.

Fabricant J. 1998. The early history of infectious bronchitis. *Avian Diseases*, **42**(4): 648−650.

Gao GF. 2018. From "A"IV to "Z"IKV: attacks from emerging and re-emerging pathogens. *Cell*, **172**(6): 1157−1159.

Guo H, Hu B, Si HR, et al. 2021. Identification of a novel lineage bat SARS-related coronaviruses that use bat ACE2 receptor. *Emerging Microbes & Infections*, **10**(1): 1507−1514.

Hastie KM, Li HY, Bedinger D, et al. 2021. Defining variant-resistant epitopes targeted by SARS-CoV-2 antibodies: a global consortium study. *Science*, **374**(6566): 472−478.

He QW, Wu LL, Xu ZP, et al. 2023. An updated atlas of antibody evasion by SARS-CoV-2 Omicron sub-variants including BQ.1.1 and XBB. *Cell Reports Medicine*, **4**(4): 100991.

Hu Y, Liu KF, Han P, et al. 2023. Host range and structural analysis of bat-origin RshSTT182/200 coronavirus binding to human ACE2 and its animal orthologs. *The EMBO Journal*, **42**(4): e111737.

Huang M, Wu LL, Zheng AQ, et al. 2022. Atlas of currently available human neutralizing antibodies against SARS-CoV-2 and escape by Omicron sub-variants BA. 1/BA. 1.1/BA. 2/BA. 3. *Immunity*, **55**(8): 1501−1514.e3.

Jia YF, Niu S, Hu Y, et al. 2022. Cross-reaction of current available SARS-

CoV-2 MAbs against the pangolin-origin coronavirus GX/P2V/2017. *Cell Reports*, **41**(11): 111831.

Ksiazek TG, Erdman D, Goldsmith CS, et al. 2003. A novel coronavirus associated with severe acute respiratory syndrome. *The New England Journal of Medicine*, **348**(20): 1953−1966.

Lam TTY, Jia N, Zhang YW, et al. 2020. Identifying SARS-CoV-2-related coronaviruses in Malayan pangolins. *Nature*, **583**(7815): 282−285.

Liu HH, Wu LL, Liu B, et al. 2023. Two pan-SARS-CoV-2 nanobodies and their multivalent derivatives effectively prevent Omicron infections in mice. *Cell Reports Medicine*, **4**(2): 100918.

Liu KF, Pan XQ, Li LJ, et al. 2021a. Binding and molecular basis of the bat coronavirus RaTG13 virus to ACE2 in humans and other species. *Cell*, **184**(13): 3438−3451.e10.

Liu YH, Hu GW, Wang YY, et al. 2021b. Functional and genetic analysis of viral receptor ACE2 orthologs reveals a broad potential host range of SARS-CoV-2. *Proceedings of the National Academy of Sciences of the United States of America*, **118**(12): e2025373118.

Murakami S, Kitamura T, Suzuki J, et al. 2020. Detection and characterization of bat sarbecovirus phylogenetically related to SARS-CoV-2, Japan. *Emerging Infectious Diseases*, **26**(12): 3025−3029.

Niu S, Wang J, Bai B, et al. 2021. Molecular basis of cross-species ACE2 interactions with SARS-CoV-2-like viruses of pangolin origin. *The EMBO Journal*, **40**(16): e107786.

Otwinowski Z, Minor W. 1997. Processing of X-ray diffraction data collected in oscillation mode. *Methods in Enzymology*, **276**: 307−326.

Pedersen NC, Evermann JF, McKeirnan AJ, et al. 1984. Pathogenicity studies of feline coronavirus isolates 79–1146 and 79–1683. *American Journal of Veterinary Research*, **45**(12): 2580−2585.

Peng MS, Li JB, Cai ZF, et al. 2021. The high diversity of SARS-CoV-2-related coronaviruses in pangolins alerts potential ecological risks. *Zoological Research*, **42**(6): 834−844.

Pensaert MB, de Bouck P. 1978. A new coronavirus-like particle associated with diarrhea in swine. *Archives of Virology*, **58**(3): 243−247.

Sharun K, Dhama K, Pawde AM, et al. 2021. SARS-CoV-2 in animals: potential for unknown reservoir hosts and public health implications. *Veterinary Quarterly*, **41**(1): 181−201.

Shi JZ, Wen ZY, Zhong GX, et al. 2020. Susceptibility of ferrets, cats, dogs, and other domesticated animals to SARS-coronavirus 2. *Science*, **368**(6494): 1016−1020.

Starr TN, Zepeda SK, Walls AC, et al. 2022. ACE2 binding is an ancestral and evolvable trait of sarbecoviruses. *Nature*, **603**(7903): 913−918.

Temmam S, Vongphayloth K, Baquero E, et al. 2022. Bat coronaviruses related to SARS-CoV-2 and infectious for human cells. *Nature*, **604**(7905): 330−336.

Wacharapluesadee S, Tan CW, Maneeorn P, et al. 2021. Evidence for SARS-CoV-2 related coronaviruses circulating in bats and pangolins in Southeast Asia. *Nature Communications*, **12**(1): 972.

Wang QH, Zhang YF, Wu LL, et al. 2020. Structural and functional basis of SARS-CoV-2 entry by using human ACE2. *Cell*, **181**(4): 894−904.e9.

Wang ZL, Huang GP, Huang MP, et al. 2023. Global patterns of phylogenetic diversity and transmission of bat coronavirus. *Science China Life sciences*, **66**(4): 861−874.

Weiner LP. 1973. Pathogenesis of demyelination induced by a mouse hepatitis. *Archives of Neurology*, **28**(5): 298−303.

Williams CJ, Headd JJ, Moriarty NW, et al. 2018. MolProbity: more and better reference data for improved all-atom structure validation. *Protein Science*, **27**(1): 293−315.

Wong G, Bi YH, Wang QH, et al. 2020. Zoonotic origins of human coronavirus 2019 (HCoV-19 / SARS-CoV-2): why is this work important?. *Zoological Research*, **41**(3): 213−219.

Wu LL, Chen Q, Liu KF, et al. 2020. Broad host range of SARS-CoV-2 and the molecular basis for SARS-CoV-2 binding to cat ACE2. *Cell Discovery*, **6**: 68.

Wu LL, Zheng AQ, Tang YM, et al. 2023. A pan-coronavirus peptide inhibitor prevents SARS-CoV-2 infection in mice by intranasal delivery. *Science China Life sciences*,doi: 10. 1007/s11427-023-2410-5.

Xiao KP, Zhai JQ, Feng YY, et al. 2020. Isolation of SARS-CoV-2-related coronavirus from Malayan pangolins. *Nature*, **583**(7815): 286−289.

Zaki AM, van Boheemen S, Bestebroer TM, et al. 2012. Isolation of a novel coronavirus from a man with pneumonia in Saudi Arabia. *The New England Journal of Medicine*, **367**(19): 1814−1820.

Zhou H, Chen X, Hu T, et al. 2020a. A novel bat coronavirus closely related to SARS-CoV-2 contains natural insertions at the S1/S2 cleavage site of the spike protein. *Current Biology*, **30**(11): 2196−2203.e3.

Zhou H, Ji JK, Chen X, et al. 2021. Identification of novel bat coronaviruses sheds light on the evolutionary origins of SARS-CoV-2 and related viruses. *Cell*, **184**(17): 4380−4391.e14.

Zhou P, Yang XL, Wang XG, et al. 2020b. A pneumonia outbreak associated with a new coronavirus of probable bat origin. *Nature*, **579**(7798): 270−273.

Zhu N, Zhang DY, Wang WL, et al. 2020. A novel coronavirus from patients with pneumonia in China, 2019. *The New England Journal of Medicine*, **382**(8): 727−733.